Enhancing Power Grid Resilience Against Typhoon Disasters by Coordinated Scheduling of Source-Network-Load

Heng Zhang, *Member, IEEE*, Shenxi Zhang, *Senior Member, IEEE*, Fangping Chen, Zheng Li, Haozhong Cheng, Gang Li, and Xiaohu Zhang

***Abstract*—To enhance the resilience of power grids against typhoon disasters, this study proposes a novel preventive scheduling method by coordinating source, network, and load resources. An evaluation index for unexpected load shedding that considers the importance of load is provided on the basis of the utility function and employed as the objective function. Moreover, the piecewise function based objective function is transformed into a mixed-integer linear formulation by introducing auxiliary variables with clear physical meanings. The startup and shutdown arrangements of units and the optimal scheduling of their outputs, as well as the opening and closing of line switches, for protecting the power supply of important loads and various demand-side management measures are comprehensively modeled. In response to the difficulty in solving the problem caused by numerous factors considered in the model, an identification method for variable and constraint reduction by narrowing the range of switchable lines is proposed to verify the effectiveness of the switchable lines in optimal transmission switching (OTS) in reducing the congestion caused by typhoon disasters. The proposed method is applied to the modified IEEE two-area system and the IEEE-118 system. Results indicate that the utility function based collaborative preventive scheduling method can effectively reduce the loss of important loads during disasters, without excessively cutting off other loads, compared with the widely used load shedding based method. Furthermore, the model dimensionality reduction method based on the effectiveness identification of switchable lines can greatly improve the solving efficiency with on decrease in the accuracy.**

***Index Terms*—Load management, optimal transmission switching, preventive scheduling, typhoon disasters, unit commitment.**

Manuscript received 31 March 2023; revised 22 July 2023; accepted 12 September 2023. Date of publication 25 September 2023; date of current version 18 January 2024. Paper 2023-PSEC-0418.R1, presented at the 2022 IEEE/IAS Industrial and Commercial Power System Asia, Shanghai, China, Jul. 08–11, and approved for publication in the IEEE TRANSACTIONS ON INDUSTRY APPLICATIONS by the Power Systems Engineering Committee of the IEEE Industry Applications Society [DOI: 10.1109/ICPSAsia55496.2022.9949900]. This work was supported in part by the National Natural Science Foundation of China under Grants U1966206, 52177099, and 52307120, in part by the State Grid Corporation of China under Grant SGHD0000GHJS2200346, and in part by Shanghai Rising-Star Program under Grant 23QA1405400. *(Corresponding author: Shenxi Zhang.)*

Heng Zhang, Shenxi Zhang, and Haozhong Cheng are with the Key Laboratory of Control of Power Transmission and Conversion, Ministry of Education, Shanghai Jiao Tong University, Shanghai 200240, China (e-mail: zhangheng_sjtu@sjtu.edu.cn; willzsx@sjtu.edu.cn; hzcheng@sjtu.edu.cn).

Fangping Chen is with Wukong Lab, IKINGTEC Company Ltd., Beijing 100871, China (e-mail: 3175195063@qq.com).

Zheng Li is with State Grid Jiangsu Electric Power Research Institute, Nanjing 211103, China (e-mail: yuanz_tju@126.com).

Gang Li and Xiaohu Zhang are with the East China Branch of State Grid Corporation, Shanghai 200240, China (e-mail: 75149272@qq.com; 374733536@qq.com).

Color versions of one or more figures in this article are available at https://doi.org/10.1109/TIA.2023.3318566.

Digital Object Identifier 10.1109/TIA.2023.3318566

NOMENCLATURE

Sets and Parameters

t	Index of time periods.
g	Index of generators.
e	Index of BESSs.
Ω	Set of generators.
Γ	Set of transmission lines.
E	Set of BESSs.
Ω_b	Set of generators at bus.
Ξ	Set of bus.
E_b	Set of BESSs at bus b.
$\mathrm{T_D}$	The total scheduling periods.
$\mathrm{N_G}$	The total number of generators.
$\mathrm{N_b}$	The total number of buses.
$p_{b,t}$	Active load of bus b.
$B_{l(m,n)}$	Reactance of transmission line l.
$N_{\mathrm{Line}}^{\mathrm{Total}}$	The total number of transmission lines.
$N_{\mathrm{Line}}^{\mathrm{Max}}$	The maximum number of switchable lines.
$N_{\mathrm{Line},t}^{\mathrm{Outage}}$	The number of fault lines.
$N_{\mathrm{Line}}^{\mathrm{NOTS}}$	The number of lines not involved in OTS.
$P_g^{\mathrm{G,min}}$	Minimum output of generator g.
$P_g^{\mathrm{G,max}}$	Maximum output of generator g.
δ_g^{up}	Ramping-up rates of generator g.
δ_g^{down}	Ramping-down rates of generator g.
$Dt_{g,t-1}^{\mathrm{n}}$	Continuous start time of generator g.
$Dt_{g,t-1}^{\mathrm{f}}$	Continuous stop time of generator g.
ϖ_g^{on}	Minimum shut-up periods of generator g.
ϖ_g^{off}	Minimum shut-down periods of generator g.
E_e^{Ini}	Initial electric energy of BESSs.
η_e^{eC}	Charge efficiency of BESSs.
η_e^{eD}	Discharge efficiency of BESSs.
$P_e^{\mathrm{cESS,min}}$	Minimum charge rates of BESSs.
$P_e^{\mathrm{dESS,min}}$	Minimum discharge rates of BESSs.
$P_e^{\mathrm{cESS,max}}$	Maximum charge rates of BESSs.
$P_e^{\mathrm{dESS,max}}$	Maximum discharge rates of BESSs.
E_e^{min}	Minimum remaining capacity of BESSs.

$E_e^{\max}$	Maximum remaining capacity of BESSs.
$PL_{l(m,n)}^{\max}$	Transmission capacity of line l.
θ_t^{ref}	Reference phase angle of the system.

Variables

$p_{b,t}^{\mathrm{LS}}$	Load shedding at bus b.
$P_{g,t}^{\mathrm{G}}$	Output of generator g.
$f_{l(m,n),t}$	Active power flow in transmission line l.
$X_{l(m,n),t}$	Working states of line l.
$P_{e,t}^{\mathrm{eC}}$	Charging power of BESSs.
$P_{e,t}^{\mathrm{eD}}$	Discharging power of BESSs.
θ_b	Phase angle of bus b.
$u_{g,t}$	Working states of generator g.
$E_{e,t}^{\mathrm{Total}}$	Remaining electric energy of BESSs.
$E_{e,t}^{\mathrm{C}}$	Charge electric energy of BESSs.
$E_{e,t}^{\mathrm{D}}$	Discharge electric energy of BESSs.
$u_{e,t}^{\mathrm{eC}}, u_{e,t}^{\mathrm{eD}}$	Working states of BESSs.

I. Introduction

DUE to the impact of global warming, high-impact low-probability related extreme weather events, such as typhoons, occur frequently in recent years, and their intensity and frequency both show an increasing trend, bringing many challenges to the security and stability of infrastructure, especially for power systems. Typhoon can cause transmission lines outage and tower collapse, which makes power systems do not provide safe and reliable power supply. In 2014, Super Typhoon Rammasun affected 2.15 million customers in China.

The concept of "resilience" was introduced to the electric power field to cope with extreme disasters. The research on improving the resilience of power systems can be divided into three stages: prevention before disasters, resistance and absorption during disasters, and recovery after disasters. Prevention measures can be divided into two main categories. The first one pertains to operation measures. On the basis of existing equipment, system operators can improve the resilience of power systems by power generation rescheduling, topology adjustment, and demand-side management before or during extreme disasters. The second category pertains to strengthening planning measures. Planners can increase equipment redundancy or enhance the disaster resistance level of equipment to resist disasters. This study focuses on operation measures for improving power system resilience through preventive scheduling.

Preventive dispatch strategies based on unit commitment (UC) are usually considered to improve power system resilience through start-up/shutdown and re-dispatch of generators. The authors in [1] studied the multiple chain faults caused by same-origin disasters and proposed an economic scheduling model constrained by resilient indexes. In order to mitigate the impact of extreme events represented by hurricanes on the day-ahead market from the perspective of probability, the authors in [2] established a two-stage robust UC model to reduce losses brought by typhoon disasters. The authors [3] proposed an active rescheduling strategy to improve the resilience of power grids in extreme events. In view of the extreme scenarios of renewable energy output, the authors in [4] proposed a multi-area UC model to improve the mutual reserve capacity of the system by using multi-area interconnection. The authors in [5] proposed a framework to boost power system resilience based on a two-stage robust optimization method, including situation awareness combined with resilience enhancement, power rescheduling in prevention and emergency situations, demand side management, and other measures. A coordinated optimization framework for power system recovery dispatch that met the requirements of priority and network constraints was proposed in [6], which modeled the post-storm recovery process as a scheduling problem under the constraints of available equipment and fuel. The above literature mainly studies preventive scheduling strategies for improving resilience from the perspective of startup and shutdown schemes and rescheduling of power generators.

Although integrating OTS into UC introduces binary variables and increases the computing burden, its excellent effects on mitigating transmission congestion and improving operating economy have attracted increasing attention [7], [8]. Recently, OTS has also been used as a means to enhance power system resilience by adjusting the power system topology through the opening and closing of transmission line switches [9]. An investment optimization approach was proposed in [8] with the aim of minimizing the total amount of load shedding over the recovery stage to resist extreme weather events by deciding optimal operating strategies of generators and transmission lines, and investment strategies. Hurricane information was predicted based on the weather forecast, and a structural model was established for transmission lines and towers to evaluate the influence of wind speed on their failure probability. On this basis, a UC-based preventive scheduling method to enhance power grid resilience with security constraints was proposed in [10]. OTS was introduced as one of the means to mitigate the geomagnetic disturbance effects on power systems, and a parallel solution approach was designed to reduce the computational complexity in [11]. A two-stage robust optimization based resilience response framework, which included preventive response and emergency response with the consideration of generator re-dispatch, optimal transmission switching and load shedding, was presented in [12], and a customized nested column-and-constraint generation decomposition method was provided to solve the complicated problem. OTS based on bilevel optimization was used to reduce cyber-physical attacks damages in [13].

UC is already very complex and faces serious solving efficiency challenges. With the introduction of OTS into UC, the operating status of transmission lines, similar to the operating status of generators, needs to be characterized by binary variables, which requires optimization at each time period. Therefore, the solution method faces even more severe challenges. Although OTS has been used in disaster preventative scheduling, researchers have focused on the design of solution algorithms to improve solving efficiency and have rarely considered efficiency improvement from the perspective of dimensionality reduction. Moreover, recent studies have considered OTS from the perspective of the entire system lines, but research on the identification of the effectiveness of OTS switchable lines has not been conducted.

In addition to generation redispatch and dynamic adjustment of transmission network topology, optimization of load operation is also one of the important measures used to enhance power

system resilience, and commonly used measures include load transferring, load shedding, load shifting, et al. [14]. Interruptible load was used to boost the resilience of electric distribution systems in [15]. Load shifting along with distributed energy resources and reconfiguration was employed to enhance the resilience in smart grids based on a multi-objective optimization framework in [16]. Demand response programs in multi-energy microgrids was proposed for operation and resiliency optimization in [17]. Energy conversion used as a new means for demand response was presented to improve both resilience and reliability of a regional integrated energy system in [18]. According to the abovementioned state-of-the-art review, resilience enhancement methods for load-side measures are mainly applied to distribution grids, microgrids, and integrated energy systems. Existing studies also usually consider only interruptible or shiftable loads and rarely model multiple load management measures in an integrated manner. Although load control is not directly realized at the transmission level, the load composition in transmission substations is diverse. Transmission system operators could perform optimization of load operation, in which the specific implementation is done at a lower voltage level, such as distribution grids.

The analysis above indicates that although many studies have been conducted to enhance power system resilience from the perspectives of the source, network, and load, preventive scheduling methods that consider coordinated source–network–load resources still need further in-depth research. Research gaps still exist. Compared with existing methods, the novelty of the proposed method lies in three aspects: 1) Unlike existing methods that improve problem solving efficiency from an algorithmic perspective, we propose a method for identifying the effectiveness of switchable lines, fundamentally reducing the number of variables and constraints in the model and thereby improving the solving efficiency. To the best of the authors' knowledge, this is the first study to propose an identification method for OTS line validity. 2) In comparison with existing studies that usually consider only interruptible or shiftable loads and rarely model multiple load management measures in an integrated manner, we comprehensively consider the collaboration between multiple demand side management methods in preventive scheduling at the transmission network level. In addition to commonly used interruptible loads, transferable and shiftable loads are all modeled. 3) We fully consider the role and mechanism of different resources in improving resilience compared with existing literature. In the proposed model, power sources, transmission lines, and multiple demand side management measures are simultaneously coordinated. Moreover, the utility function of each bus load shedding loss is taken as the objective function of the preventive scheduling model rather than the widely used penalty costs or weighted load shedding loss with a linear functional relationship with the total amount of load shedding.

In view of the inadequacy of existing research, this study proposes a preventive scheduling method based on UC that considers demand-side management measures, transmission topology optimization, operating status, and re-dispatch of generators. It aims to improve power system resilience and reduce the effects of typhoon disasters on power supply for important loads by coordinating the flexible operation of source–network–load resources. The contributions of this work are as follows:

1) We provide a new perspective on model dimensionality reduction for preventive scheduling optimization problems considering OTS strategies. An identification method for verifying the effectiveness of switchable lines in OTS is proposed. The proposed method can effectively reduce the number of lines in OTS by narrowing the range of switchable lines and thus improve solving efficiency on the premise of ensuring the accuracy of the solution. The simulation results show that switching only the lines near the fault location can effectively improve the supply capacity of important loads and reduce disaster losses. This technique will greatly decrease the number of variables and constraints introduced by OTS, especially in preventive scheduling models that consider hourly unit startup and shutdown, which can greatly improve solution efficiency while ensuring accuracy.
2) We integrate various demand side management measures into the preventive scheduling model. Through collaborating with transferable, shiftable, and interruptible load strategies, the supply capacity of important loads during disasters can be effectively improved. Overall, compared with the use of transferable and shiftable loads, the utilization of interruptible loads is the most accurate and effective method.
3) A novel model for improving the resilience of power systems under typhoon disasters by coordinating source–network–load resources is proposed. In terms of the objective function, the utility function is used to represent the losses of each bus load shedding, which effectively takes into account the nonlinear relationship between the amount of load shedding and losses. In terms of constraints, power generation on/off status and output rescheduling, transmission network line switching and transferable loads, shiftable loads, and interruptible loads are fully considered. We demonstrate that collaborative scheduling among multiple resources can effectively reduce disaster losses. In addition, the utility function based load shedding can effectively ensure the power supply of important loads, and no significant difference in the overall load shedding amount will occur.

The rest of the article is organized as follows. Comprehensive load management strategies are modeled in Section II. Section III proposes the presentative scheduling method considering UC, OTS, and demand side management strategies. Case studies are presented in Section IV to show the effectiveness of the method, and conclusions are made in Section V.

II. Comprehensive Load Management Strategies

Transferable and shiftable loads belong to planned management measures. Interruptible load is a method for contractual management, and its specific call time is unknown and implemented in accordance with actual situations. Conventional load, although it can be removed, has different costs, and the

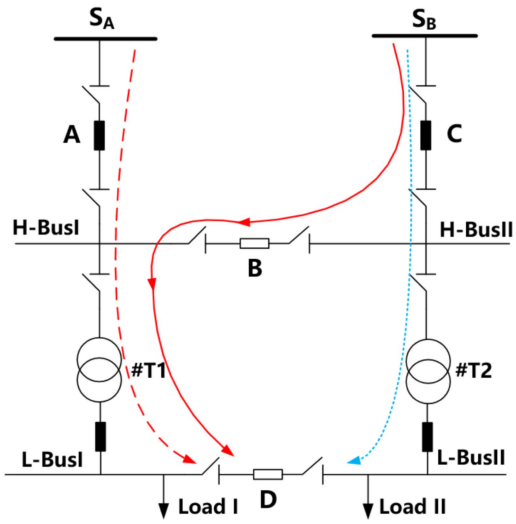

Fig. 1. Schematic diagram of load transferring.

amount of load shedding and its costs do not always show a linear relationship. For entities requiring important load, such as government departments and hospitals, uninterrupted power supply should be ensured.

Power system operators make operating plans for risky areas based on the forecast information of typhoons. Load transferring is the first consideration of a demand-side management strategy, and it has the least impact on customers. Shifting loads from buses with supply shortages to others with sufficient supply does not change the electricity plans of customers. Moreover, load shifting can change consumers' electricity plans, but it does not affect the total power demand of the load. Load interruption, which often occurs in agreement with the power system company, can be implemented during difficult periods of power supply. Shedding conventional load causes direct losses, with the largest one occurring during preventive scheduling. However, economic compensation can offset part of the losses. Notably, important loads, whose supply must be guaranteed, may cause political, life safety-related, and social problems.

A. Transferable Load Strategy

In modern power systems, a substation is usually supplied by different buses with power from different sources to improve the reliability. In Fig. 1, buses S_A and S_B have different power sources. Assuming that under normal conditions, loads I and II are supplied from the power source of bus S_A when switches B and C are open and switch D is closed. When the power supply capacity of bus S_A decreases due to a typhoon disaster, operators can open switches B and D and close C so that load I is supplied by S_A and load II is supplied by S_B to realize load transfer. The power supply path is shown as red and blue dashed lines in Fig. 1.

When bus S_A completely loses its power supply capacity, loads I and II can be completely supplied by bus S_B by disconnecting switch A, closing switches C and B, and disconnecting D or by disconnecting switch A, closing switches C and D, and disconnecting B. The red solid line in Fig. 1 gives a path of power supply from bus S_B. Based on the above analysis, for any bus b, at moment t, its load transferring operation can be characterized as:

$$0 \le p_{b,t}^{\mathrm{Trans,out}} \le \xi * p_{b,t};\ \forall b \in \Xi, \forall t \tag{1}$$

$$\sum_{c \in \Xi_b^{\mathrm{Trans}}} p_{c,t}^{\mathrm{Trans,in}} = p_{b,t}^{\mathrm{Trans,out}};\ \forall b \in \Xi, \forall t \tag{2}$$

$$p_{c,t}^{\mathrm{Trans,in}} \ge 0;\ \forall b, c, t \tag{3}$$

Where, $p_{b,t}^{\mathrm{Trans,out}}$ denotes the amount of load transferred out from bus b at moment t; ξ denotes the maximum allowable load transfer ratio; Ξ_b^{Trans} denotes the set available for load transfer from bus b; c denotes the bus number in the load transfer set; $p_{c,t}^{\mathrm{Trans,in}}$ denotes the amount of load transferred from other buses to bus c.

Equation (1) indicates the amount of load that can be transferred out of bus b at time t; (2) indicates that the total amount of load transferred out is equal to the load transferred into each bus, i.e., no load is lost in the process of load transferring.

B. Shiftable Load Strategy

By adjusting the time and volume of power consumption, shiftable load can flexibly realize energy consumption while meeting consumers' power demand. In reality, flexible loads are increasingly used nowadays, and the losses of load shedding that emerge when power systems suffer from typhoon disasters can be reduced by arranging the electricity demand in advance. For shiftable load at bus b, its power consumption constraint throughout the preventive scheduling cycle can be characterized as follows:

$$p_{b,t}^{\mathrm{Shift}} = p_{b,t} - p_{b,t}^{\mathrm{Shift,out}} + p_{b,t}^{\mathrm{Shift,in}};\ \forall b, t \tag{4}$$

$$0 \le p_{b,t}^{\mathrm{Shift,out}} \le \tau * p_{b,t};\ \forall b, t \tag{5}$$

$$0 \le p_{b,t}^{\mathrm{Shift,in}} \le \tau * p_{b,t};\ \forall b, t \tag{6}$$

$$\sum_t p_{b,t}^{\mathrm{Shift,out}} = \sum_t p_{b,t}^{\mathrm{Shift,in}};\ \forall b, t \tag{7}$$

Where $p_{b,t}^{\mathrm{Shift}}$ denotes the remaining load at bus b at moment t, i.e., the actual load at bus b after partial load shifting; $p_{b,t}^{\mathrm{Shift,out}}$ denotes the amount of load moved out of bus b at moment t; $p_{b,t}^{\mathrm{Shift,in}}$ denotes the amount of load moved into bus b at moment t; τ denotes the ratio that load shifting can be performed.

Equation (4) indicates the load remaining at bus b after load shifting; (5) and (6) indicate the volume that load shifting is allowed; (7) indicates the total amount of load in the bus before and after load shifting is constant throughout the preventive scheduling cycle.

C. Interruptible Load Strategy

Interruptible load is widely used in different countries to maintain system security and stability. Interruptible load can be shed to ensure the supply of other important loads when a power shortage occurs in power systems. For buses containing interruptible load, the loss of load shedding can be characterized

by the segmentation function:

$$p_{b,t}^{\text{loss}} = \begin{cases} 0 & 0 \le p_{b,t}^{\text{LS}} \le \upsilon * p_{b,t} \\ U_b\left(p_{b,t}^{\text{LS}} - \upsilon * p_{b,t}\right) & p_{b,t}^{\text{LS}} > \upsilon * p_{b,t} \end{cases} \quad \forall b,t \tag{8}$$

Where $p_{b,t}^{\text{loss}}$ denotes loss of load shedding; υ denotes interruptible load share; $p_{b,t}^{\text{LS}}$ denotes total load shedding volume; $U_b(*)$ denotes loss function of load shedding.

Equation (8) indicates that an unplanned outage loss arises only when the amount of load shedding exceeds the limited volume of interruptible load. The segment function shown in (8) characterizing the losses of load shedding is difficult to embed into the preventative scheduling model directly. Considering the special structure of (8), when the total amount of load shedding is smaller than the limited volume of interruptible load, the loss of load shedding is zero. For this reason, with the introduction of auxiliary variables $p_{b,t}^{\text{IL}}$ and $p_{b,t}^{\text{NLS}}$, the total amount of load shedding can be expressed as:

$$p_{b,t}^{\text{LS}} = p_{b,t}^{\text{IL}} + p_{b,t}^{\text{NLS}} \quad \forall b,t \tag{9}$$

$$0 \le p_{b,t}^{\text{IL}} \le \upsilon * p_{b,t} \quad \forall b,t \tag{10}$$

$$0 \le p_{b,t}^{\text{NLS}} \le (1-\sigma) * p_{b,t} \quad \forall b,t \tag{11}$$

Where σ represents the share of important loads which are not allowed to be shed. Since interruptible load is not taken as unplanned outage losses, then (8) can be modified to

$$p_{b,t}^{\text{loss}} = U_b(p_{b,t}^{\text{NLS}}) \forall b,t \tag{12}$$

Auxiliary variables $p_{b,t}^{\text{IL}}$ and $p_{b,t}^{\text{NLS}}$ denote the interruptible load volume and load shedding volume of bus b at time t, respectively. Among them, only the normal load shedding accounts for the unplanned outage losses.

III. Preventive Scheduling Based on Unit Commitment

A. OTS Method Combined With Switchable Lines Effectiveness Identification

OTS is often associated with the occurrence of congestion, and can be used to eliminate transmission congestion by actively disconnecting transmission lines to reduce operating costs [19], [20]. It employs the difference in the operating costs of different generators and prioritizes the generators with low operating costs by adjusting the transmission network topology. Thus, the total operating costs can be reduced. The losses brought by shedding the same amount of load differ because of the different importance of loads. Therefore, theoretically, the transmission network topology can be optimized to change the distribution of power flow, serve users with high load priority, and reduce the losses of load shedding.

Research on OTS is usually based on the single period optimal power flow method. However, with the introduction of OTS into the multi-period UC model in this study, to achieve consistency with the later description of the time scale, this section provides the OTS model in a multi-period form. At each time period, the transmission line can be disconnected. The duration interval of the disconnected line is set to 1h. That is, at the next time $t+1$, the line that is disconnected at time t can resume operation or continue to remain disconnected. Considering the goal of minimizing the total amount of load shedding, the model of OTS based on the direct current optimal power flow is as follows:

$$\min \sum_{t=1}^{\text{T}_\text{D}} \sum_{b=1}^{\text{N}_\text{b}} p_{b,t}^{\text{LS}} \tag{13}$$

$$\text{s.t.} \sum_{\forall g \in \Omega_b} P_{g,t}^{\text{G}} + \sum_{\forall m,n \in \Xi_b} f_{l(m,n),t} = p_{b,t} - p_{b,t}^{\text{LS}};\ \forall b \in \Xi, \forall t \tag{14}$$

$$f_{l(m,n),t} + B_{l(m,n)}\left(\theta_{m,t} - \theta_{n,t}\right) = 0\ \forall l(m,n) \in \Gamma \backslash \left(\Gamma^0 \cup \Gamma^k\right), \forall t \tag{15}$$

$$\left| \frac{f_{l(m,n),t}}{B_{l(m,n)}} + \left(\theta_{m,t} - \theta_{n,t}\right) \right| \le \left(1 - X_{l(m,n),t}\right) * M;\ \forall l(m,n) \in \Gamma^k, \forall t \tag{16}$$

$$\left| f_{l(m,n),t} \right| \le PL_{l(m,n)}^{\max};\ \forall l(m,n) \in \Gamma \backslash \left(\Gamma^0 \cup \Gamma^k\right), \forall t \tag{17}$$

$$\left| f_{l(m,n),t} \right| \le PL_{l(m,n)}^{\max} * X_{l(m,n),t};\ l(m,n) \in \Gamma^k, \forall t \tag{18}$$

$$X_{l(m,n),t} \in \{0,1\};\ \forall l(m,n) \in \Gamma^k, \forall t \tag{19}$$

$$N_{\text{Line}}^{\text{Total}} - N_{\text{Line}}^{\text{NOTS}} - N_{\text{Line},t}^{\text{Outage}} - \sum_{\forall l(m,n) \in \Gamma^k} X_{l(m,n),t} \le N_{\text{Line}}^{\text{Max}}; \forall t \tag{20}$$

$$P_g^{\text{G,min}} \le P_{g,t}^{\text{G}} \le P_g^{\text{G,max}};\ \forall g \in \Omega, \forall t \tag{21}$$

$$\theta_t^{ref} = 0\ \forall t \tag{22}$$

Equation (14) represents nodal power balance; (15) and (16) represent power flow constraints with/without participating in OTS; (17) and (18) are maximum transmission capacity constraints of lines with/without participating in OTS; (19) represents whether the transmission lines can be switched off actively; (20) represents the maximum number of switchable lines of each time period to avoid a significant decrease in power system reliability if too many transmission lines are switched off; (21) represents the minimum and maximum output of generators; (22) is the reference bus angle.

For power systems in normal operation conditions, transmission congestion does not usually occur. However, when power systems are affected by typhoon disasters and some transmission lines fail, transmission congestion problems occur locally in power system. By considering the OTS of all lines in a power system, the most effective measures (when to switch off/on some transmission lines) can be identified. For large-scale power systems, considering all lines may increase the computing burden because OTS introduces many binary variables to represent the operating status of transmission lines. Therefore, a novel strategy to limit the number of transmission lines involved in OTS is studied in this work, and the set of switchable transmission lines is shown in (15)∼(19).

Let Γ^k denote the set of non-faulty transmission lines with k-order correlation with the faulty line and Ξ_{outage}^k denote the

set of all buses at both ends of the faulty transmission lines. The k-order correlation is obtained recursively from the non-faulty transmission lines directly connected to the buses at both ends of the faulty transmission lines. In particular, when k = 0, Γ^0 represents the set of the faulty transmission lines, and Ξ^0_{outage} represents the set of all buses at both ends of the faulty transmission lines.

Γ^1 represents the set of all transmission lines that are directly connected to the faulty transmission lines. The buses of all transmission lines in Γ^1 form the set Ξ^1_{outage}.

$$\Gamma^1 = \left\{ l(m,n) | \left(\forall m,n \in \Xi^0_{\text{outage}}\right) \cup \left(l(m,n) \notin \Gamma^0\right) \right\} \quad (23)$$

Similarly, Γ^2 represents the set of all transmission lines that are directly connected to the transmission lines in Γ^1 and do not belong to the faulty transmission line set Γ^0.

$$\Gamma^2 = \left\{ l(m,n) | \left(\forall m,n \in \Xi^1_{\text{outage}}\right) \cup \left(l(m,n) \notin \Gamma^0\right) \right\} \quad (24)$$

Analogously, we can get $\Gamma^k (k > 1)$

$$\Gamma^k = \left\{ l(m,n) | \left(\forall m,n \in \Xi^{k-1}_{\text{outage}}\right) \cup \left(l(m,n) \notin \Gamma^0\right) \right\} \quad (25)$$

By limiting the value of *k*, the number of transmission lines involved in OTS can be effectively reduced, thus reducing the number of integer variables in OTS model, achieving the purpose of model refinement characterization and improving solving efficiency of model.

B. Preventive Scheduling Model Based on Minimum Load Shedding

Most existing preventive scheduling models aim to minimize the total amount of load shedding. They take the minimum load shedding of power systems during typhoon disasters as the objective function and consider the constraints of generator start-up and shutdown, power flow equation, and so on. The detailed formulation is as follows:

$$\min \sum_{t=1}^{\mathrm{T_D}} \sum_{b=1}^{\mathrm{N_b}} p^{\mathrm{LS}}_{b,t} \quad (26)$$

$$\sum_{\forall g \in \Omega_b} P^G_{g,t} + \sum_{\forall m,n \in \Xi_b} f_{l(m,n),t} + \sum_{e \in E_b} P^{eD}_{e,t} - \sum_{e \in E_b} P^{eC}_{e,t} = P_{b,t} - P^{LS}_{b,t};\ \forall b \in \Xi, \forall t \quad (27)$$

$$f_{l(m,n),t} + B_{l(m,n),t}\left(\theta_{m,t} - \theta_{n,t}\right) = 0;\ \forall l(m,n) \in \Gamma, \forall t \quad (28)$$

$$u_{g,t} P^{\mathrm{G,min}}_g \le P^{\mathrm{G}}_{g,t} \le u_{g,t} P^{\mathrm{G,max}}_g; \forall g \in \Omega, \forall t \quad (29)$$

$$P^{\mathrm{G}}_{g,t} - P^{\mathrm{G}}_{g,t-1} \le \delta^{\mathrm{up}}_g; \forall g \in \Omega, \forall t \quad (30)$$

$$P^{\mathrm{G}}_{g,t-1} - P^{\mathrm{G}}_{g,t} \le \delta^{\mathrm{down}}_g; \forall g \in \Omega, \forall t \quad (31)$$

$$\left(u_{g,t-1} - u_{g,t}\right)\left(Dt^{\mathrm{n}}_{g,t-1} - \varpi^{\mathrm{on}}_g\right) \ge 0; \forall g \in \Omega, \forall t \quad (32)$$

$$\left(u_{g,t} - u_{g,t-1}\right)\left(Dt^{\mathrm{f}}_{g,t-1} - \varpi^{\mathrm{off}}_g\right) \ge 0; \forall g \in \Omega, \forall t \quad (33)$$

$$E^{\mathrm{Total}}_{e,t} = E^{\mathrm{Ini}}_e + \sum_{m=1}^{N_T} E^{\mathrm{C}}_{e,m} + \sum_{m=1}^{N_T} E^{\mathrm{D}}_{e,m}; \forall e,t; N_T = 1,2,3\ldots t \quad (34)$$

$$E^{\mathrm{C}}_{e,t} = \eta^{\mathrm{eC}}_e \int_{\Delta t} P^{\mathrm{eC}}_{e,t} dt; \forall e,t \quad (35)$$

$$E^{\mathrm{D}}_{e,t} = \eta^{\mathrm{eD}}_e \int_{\Delta t} P^{\mathrm{eD}}_{e,t} dt; \forall e,t \quad (36)$$

$$u^{\mathrm{eD}}_{e,t} P^{\mathrm{dESS,min}}_e \le P^{\mathrm{eD}}_{e,t} \le u^{\mathrm{eD}}_{e,t} P^{\mathrm{dESS,max}}_e; \forall e,t \quad (37)$$

$$u^{\mathrm{eC}}_{e,t} P^{\mathrm{cESS,min}}_e \le P^{\mathrm{eC}}_{e,t} \le u^{\mathrm{eC}}_{e,t} P^{\mathrm{cESS,max}}_e; \forall e,t \quad (38)$$

$$E^{\mathrm{min}}_e \le E^{\mathrm{Total}}_{e,t} \le E^{\mathrm{max}}_e \quad \forall e,t \quad (39)$$

$$-PL^{\mathrm{max}}_{l(m,n)} \le f_{l(m,n),t} \le PL^{\mathrm{max}}_{l(m,n)};\ \ l(m,n) \in \Gamma, \forall t \quad (40)$$

$$0 \le p^{\mathrm{LS}}_{b,t} \le p_{b,t};\ \ \forall b,t \quad (41)$$

$$u^{\mathrm{eD}}_{e,t}, u^{\mathrm{eC}}_{e,t} \in \{0,1\}; \forall e \in E, \forall t \quad (42)$$

$$u_{g,t} \in \{0,1\}; \forall g \in \Omega, \forall t \quad (43)$$

$$u^{\mathrm{eD}}_{e,t} + u^{\mathrm{eC}}_{e,t} \le 1; \forall e \in E; \forall t \quad (44)$$

$$\theta^{ref}_t = 0 \quad (45)$$

(27) represents nodal power balance; (28) represents power flow equation; (29) is the output of generators; (30) and (31) are the climbing/downhill rate constraints of generators; (32) and (33) are the minimum start-up and shutdown time constraints of generators, and its linearization method can be referred to reference [21]. (34) is the equation of remaining capacities of battery energy storage systems (BESSs); (35) and (36) are the charge and discharge equation of BESSs; (37) and (38) are the charge and discharge rate constraint of BESSs; (39) is the capacity constraints of BESSs; (40) is the maximum capacities of transmission lines; (41) is the maximum load shedding of each bus; (42) and (43) are the working state variables of BESSs and generators; (44) is the charge and discharge states constraints of BESSs, that is, there can only be one state in the same period; (45) is the reference bus angle.

C. Preventive Scheduling Model Based on Load Shedding Losses Minimization

The utility function is usually used to represent the "subjective satisfaction" obtained by consumers. The utility function is introduced in this study to represent the "subjective losses" of consumers caused by typhoon disasters. For bus *b*, the losses caused by power equipment failure at time *t* can be expressed as the disaster loss utility function $U_b(p^{\mathrm{NLS}}_{b,t})$, whose values represent the importance of load and users' tolerance for disaster losses. The "S" function, exponential function, and power function are usually adopted as utility functions. In this study, the power function of the conservative utility function is used to represent disaster losses caused by typhoons. The detailed formulation is as follows:

$$U_b\left(p^{\mathrm{NLS}}_{b,t}\right) = \left(p^{\mathrm{NLS}}_{b,t}\right)^{a_b} \quad (46)$$

Where a_b represents power exponent. According to (46), the objective function (26) of the proposed preventive scheduling

model can be modified into the following form:

$$\min U_{\mathrm{SLoLS}} = \sum_{t=1}^{\mathrm{T_D}} \sum_{b=1}^{\mathrm{N_b}} U_b(p_{b,t}^{\mathrm{NLS}}) = \sum_{t=1}^{\mathrm{T_D}} \sum_{b=1}^{\mathrm{N_b}} (p_{b,t}^{\mathrm{NLS}})^{a_b} \tag{47}$$

Since the power function is with strong nonlinearity, it is difficult to solve the model directly. In this study, the piecewise linearization method is adopted to transform the objective function as follows:

$$\left(p_{b,t}^{\mathrm{NLS}}\right)^{a_b} = \sum_{i=1}^{\mathrm{N}+1} \vartheta_i \left(p_{b,t,i}^{\mathrm{NLS}}\right)^{a_b} \tag{48}$$

$$p_{b,t}^{\mathrm{NLS}} = \sum_{i=1}^{\mathrm{N}+1} \vartheta_i p_{b,t,i}^{\mathrm{NLS}} \tag{49}$$

Where $p_{b,t,i}^{\mathrm{NLS}}$ is the interpolation point; N is the number of segments;ϑ_i is the weight coefficient, which should satisfy the following constraints:

$$\begin{cases} \sum_{i=1}^{\mathrm{N}+1} \vartheta_i = 1, \vartheta_i \geq 0 \\ \vartheta_1 \leq \varsigma_1, \vartheta_{1+\mathrm{N}} \leq \varsigma_{\mathrm{N}} \\ \vartheta_j \leq \varsigma_{j-1} + \varsigma_j, \forall j \in \{2, 3, \ldots, N\} \\ \sum_{i=1}^{\mathrm{N}} \varsigma_i = 1, \forall \varsigma_i \in \{0, 1\} \end{cases} \tag{50}$$

So far, the objective function based on the power exponent expressed by the (47) has been transformed into mixed integer linear constraints. The objective function of the proposed preventive scheduling model (47)∼(50) after transformation can be obtained as follows:

$$\min \sum_{t=1}^{\mathrm{T_D}} \sum_{b=1}^{\mathrm{N_b}} \sum_{i=1}^{\mathrm{N}+1} \vartheta_i (p_{b,t,i}^{\mathrm{NLS}})^{a_b} + \rho \sum_{t=1}^{\mathrm{T_D}} \sum_{b=1}^{\mathrm{N_b}} \times \left(p_{b,t}^{\mathrm{Trans,in}} + p_{b,t}^{\mathrm{Trans,out}} + p_{b,t}^{\mathrm{Shift,in}} + p_{b,t}^{\mathrm{Shift,out}} + p_{b,t}^{\mathrm{Inter}}\right) \tag{51}$$

The first term of (51) represents the losses caused by unexpected load shedding, and the second term is utilized to avoid unnecessary load transfer, shifting, and interruption. ρ represents the penalty coefficient, and it can take a small value, such as 10^{-4}, to avoid the impact on unplanned load shedding. The objective function of the proposed model minimizes the losses of load shedding. Therefore, a highly realistic preventive scheduling strategy can be obtained by adding the penalty term without affecting the final generation scheduling and transmission topology optimization results.

In consideration of different load management measures, namely, transferable, shiftable, and interruptive loads, the nodal power balance constraints in (27) should be modified as follows:

$$\sum_{\forall g \in \Omega_b} P_{g,t}^{\mathrm{G}} + \sum_{\forall m,n \in \Xi_b} f_{l(m,n),s,t} + \sum_{e \in E_b} P_{e,t}^{\mathrm{eD}} - \sum_{e \in E_b} P_{e,t}^{\mathrm{eC}} = p_{b,t} + p_{b,t}^{\mathrm{Trans,in}} - p_{b,t}^{\mathrm{Trans,out}} + p_{b,t}^{\mathrm{Shift,in}} - p_{b,t}^{\mathrm{Shift,out}} - p_{b,t}^{\mathrm{IL}} - p_{b,t}^{\mathrm{NLS}}; \ \forall b \in \Xi, \forall t \tag{52}$$

In addition to (52), the other constraints are (1)∼(3), (5)∼(7), (10)∼(11), (15)∼(20), (29)∼(39), (42)∼(45), and (49)∼(50).

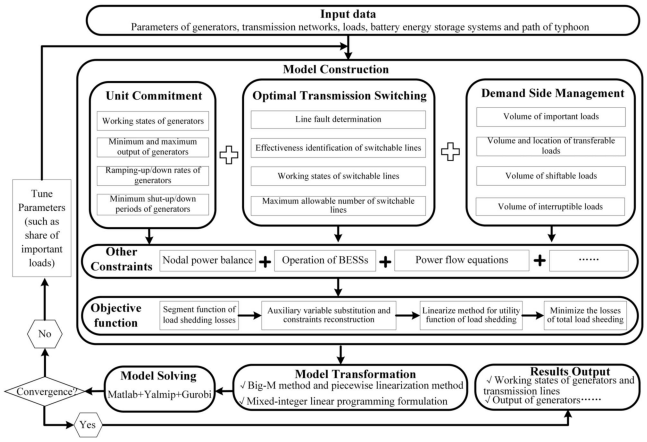

Fig. 2. Overall framework diagram of the proposed preventive scheduling method.

TABLE I
PARAMETERS VALUES OF THE MODIFIED IEEE TWO-AREA TEST SYSTEM

$P_e^{\mathrm{cESS,min}}$	0 MW/h	$E_{ini,e}$	20 MWh
$P_e^{\mathrm{dESS,min}}$	0 MW/h	$E_{e,\max}^{End}$	10 MWh
$P_e^{\mathrm{cESS,max}}$	25 MW/h	$E_{e,\min}^{End}$	50 MWh
$P_e^{\mathrm{dESS,max}}$	25 MW/h	a_b	0.25

TABLE II
INFORMATION OF THE FAULTY LINES

t	7	8	14	17
Line(s)	36-37	36-47, 35-37	43-44(2)	39-45(2)

The overall framework of the proposed method is shown in Fig. 2.

IV. EXAMPLE ANALYSIS

In order to verify the effectiveness of the proposed method, we used the modified IEEE Two-area test system and IEEE-118 system for numerical simulation and analysis. Assuming that typhoon moves along a straight path [22], and all lines on the typhoon's path are forced outage due to strong winds [23]. Bus 10 and 29 are equipped with BESSs, and parameters are shown in Table I. All programs in this article are made on Matlab using YALMIP toolkit and Gurobi solver with laptop Intel Core i5-1240P 1.70 GHz CPU and 16 GB RAM.

A. The Modified IEEE Two-Area Test System

The modified IEEE two-area test system is shown in Fig. 3. Based on reference [24], we have made modifications to the data, and it can be found in reference [25]. All generators have the ability to reach their rated power capacity within one hour. The typhoon affects the transmission lines from $t = 7$, and a total of seven lines are affected by the typhoon with forced outage faults throughout the process. The relevant fault line information is shown in Table II.

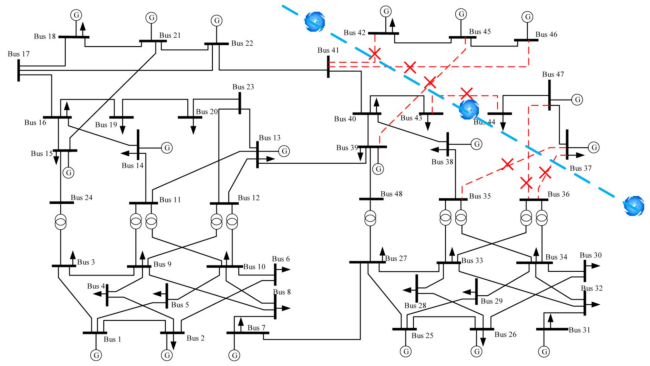

Fig. 3. Schematic diagram of the modified IEEE two-area test system.

TABLE III
PREVENTATIVE SCHEDULING RESULTS WITH DIFFERENT OBJECTIVE FUNCTIONS

σ, ξ, τ, υ	Case1		Case2	
	SLoLS	LS(MWh)	SLoLS	LS(MWh)
20%, 0, 0, 0	28.35	5112	43.29	5017
20%, 30%, 0, 0	25.19	4648	38.10	4646
20%, 30%, 5%, 0	13.80	2563	20.83	2505
20%, 30%, 5%, 5%	5.36	964	8.76	958

1) Comparison of Preventive Scheduling Methods With Different Objective: The amount of load shedding is a visual representation of the magnitude of losses brought by typhoon disasters to power systems and has been used as an objective function for preventive scheduling in many studies. However, the losses caused by load shedding at each bus of power systems do not always show a linear relationship with the amount of load shedding in practice, and the importance of loads at different buses varies. In this section, two cases are set up, and each case considers four scenarios to compare the difference in the losses caused by unexpected load shedding with different preventive scheduling methods.

Case 1: The preventive scheduling method based on the utility function proposed in this study.

Case 2: The traditional preventive scheduling approach with the minimum amount of load shedding as the objective function.

The values of SLoLS and load shedding are shown in Table III. The amount of load shedding in the two cases presents differences because of the priority levels of different bus loads and the non-linear relationship between the losses and amount of load shedding. With the fourth scenario as an example ($\sigma = 20\%$, $\xi = 30\%$, $\tau = 5\%$, $\nu = 5\%$), from the perspective of the total amount of load shedding during all the scheduling periods, Case 1 has 964 MWh, which is higher than that of Case 2 with 958 MWh; the difference is only 0.06%. However, from the perspective of the utility value, the SLoLS of Case 1 is 5.36, and that of Case 2 is 8.76; the percentage difference is 38.81%. These results indicate that considering load as equally important and adopting the amount of load shedding as the objective function cannot accurately evaluate the losses caused by typhoon disasters. Therefore, the willingness of different users to bear disaster losses must be considered when formulating prevention scheduling strategies. The results also indicate that it is not accurate and comprehensive to reflect the power outage losses caused by typhoon disasters when the load is regarded as having an equal importance and shed without any differences during typhoon disasters.

TABLE IV
SLoLS WITH DIFFERENT LOAD MANAGEMENT STRATEGIES

σ=20%, τ=υ=0		σ=20%, ξ=30%, υ=0		σ=20%, ξ=30%, τ=5%	
ξ=0	28.35	τ=0	25.19	υ=0	13.80
ξ=10%	27.08	τ=5%	13.80	υ=5%	5.36
ξ=20%	26.00	τ=10%	5.36	υ=10%	0.60
ξ=30%	25.19	τ=15%	0.60	υ=15%	0
ξ=40%	24.61	τ=20%	0	υ=20%	0

2) Impact of Integrated Demand Side Management Measures on Power System Resilience: Different load management measures have different mechanisms of reducing the power system losses caused by typhoon hazards. A sensitivity analysis is conducted in this section to investigate the effect of different demand-side management measures on reducing losses. OTS measures are not considered in this section.

Table IV shows that shiftable and interruptible loads have a more obvious impact on power system resilience compared with transferable load. With bus 39 with different demand-side management measures ($\sigma = 20\%$, $\xi = 30\%$, $\tau = 5\%$, $\nu = 5\%$) as an example, the abovementioned results show that load shifting and interruptible load measures are adopted only when some lines fail after a typhoon arrives. Load transferring occurs at $t = 17$, and the interruptible load strategy is employed at $t = 15$. In the case of shiftable load, although transmission line faults have not yet affected bus 39 load supply at the early stage (e.g., $t = 3$–15), load shifting is used at bus 39 from $t = 3$ to effectively reduce the impact of load shedding because it can be implemented throughout the whole scheduling cycle. A total of 117.79 MWh of load is transferred from $t = 16$–23 to $t = 3$–14.

SLoLS, which characterizes power system losses, decreases from 28.35 to 24.61 with a decrease of 13.19% when the transfer capability is increased from 0% to 40% of the load of buses shiftable to the adjacent buses. Similarly, while maintaining 30% transferable capability and 5% shiftable load at each bus, the losses caused by typhoon disasters are gradually reduced to 0 by increasing the volume of interruptible load. This result is due to the fact that by adjusting the temporal distribution of shiftable load throughout all the preventative scheduling periods, this load can play a role similar as that of interruptible load but without causing any load loss.

3) Analysis of OTS on Improving Power Grid Resilience: This section investigates the effect of OTS strategies on improving power system resilience to cope with typhoon disasters with/without considering OTS in two cases. Due to the small scale of the system, all lines can be switched off/on. Parameter values are shown in Table V. Figs. 4 and 5 show the output of

TABLE V
PARAMETER VALUES WITH DIFFERENT CASES

Case	σ	ξ	τ	υ	The number of switchable lines
3	20%	30%	5%	5%	3
4	20%	30%	5%	5%	0

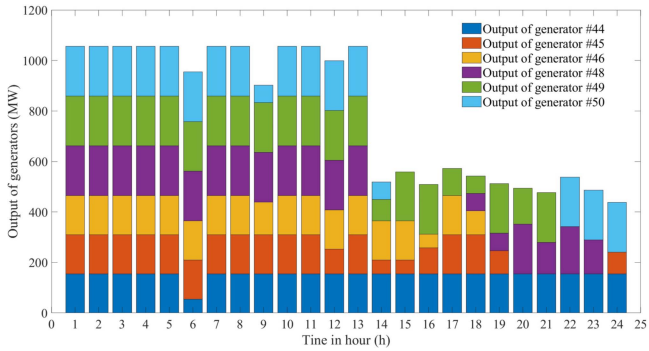

Fig. 4. Output of generators in Case 3.

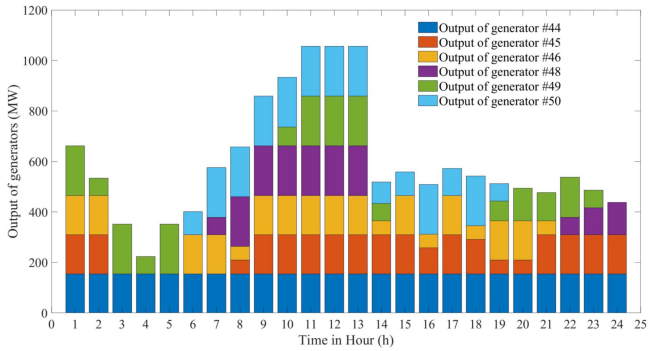

Fig. 5. Output of generators in Case 4.

TABLE VI
AMOUNT OF LOAD SHEDDING AT DIFFERENT BUSES IN CASE 3 AND CASE 4

Case	SLoLS	The amount of load shedding (MWh)
3	4.93	900
4	5.36	964

some generators in different cases, and Table VI shows the total amount of load shedding in different cases.

As shown in Figs. 4 and 5, the output of the generators at certain buses varies due to the optimization of transmission network topology. For example, the output of the generators numbered G44–G46 and G48–G50 is 19064 MWh during the whole preventive scheduling periods in Case 3, but it decreases to 14367 MWh in Case 4. In addition to the change in the total generated electric energy, the power outputs of the generators in the different cases also differ each time. The result also indicates that transmission network topology optimization during typhoon disasters by using OTS affects generators' optimal output. From the perspective of the utility function of the total disaster losses, the SLoLS in Case 4 is 5.36, whereas the SLoLS in Case 3 is only 4.93. The decrease of 8% is due to the consideration of OTS. In addition, the total amount of load shedding in Case 3 is reduced by 64 MWh compared with that in Case 4. Although the absolute amount of load shedding decreases slightly when Case 3 is compared with and Case 4, the differences is from the perspective of the utility value. OTS can effectively reduce the amount of power system load shedding, thereby reducing the losses represented by SLoLS caused by the unexpected outage of transmission lines during typhoon disasters.

TABLE VII
FAULTY LINES CAUSED BY TYPHOON DISASTERS

t	Line(s)	t	Line(s)
3	59-61	10	52-53
4	59-60	11	42-49(2)
6	63-64	12	37-40
7	56-57, 56-58	13	40-42
8	49-54(2)	14	39-40

TABLE VIII
RESULTS OF PREVENTION SCHEDULING METHODS WITH DIFFERENT OBJECTIVE FUNCTIONS

σ, ξ, τ, υ	The proposed method		Load shedding based method	
	SLoLS	LS(MWh)	SLoLS	LS(MWh)
20%, 0, 0, 0	2.38	5899	3.12	5899
20%, 30%, 0, 0	2.22	5703	3.05	5703
20%, 30%, 5%, 0	2.11	5376	2.92	5373
20%, 30%, 5%, 5%	1.76	4296	2.59	4290

B. *Modified IEEE-118 Test System*

In order to verify the effectiveness of the proposed method for large-scale power systems, this section validates the proposed method in the modified IEEE-118 test system based on the data in reference [26]. Some modified data can be found in reference [25]. All generators have the ability to reach their rated power capacity within two hours. The typhoon is still traveling in a straight line, and the transmission lines on its travel route are considered to be in fault condition. The faulty lines and their fault time are shown in Table VII. The information on parameters such as energy storage is consistent with the modified IEEE two-area test system.

1) SLoLS vs. Load Shedding: The effectiveness of the different methods, i.e., the proposed method and load shedding based method, are analyzed in terms of the total amount of load shedding and SLoLS for different scenarios. The results are presented in Table VIII.

The results in Table VIII show that the proposed method can effectively reduce the total amount of load shedding and SLoLS by using integrated demand-side management strategies. Load shedding decreases from 5899 MWh to 4296 MWh, and SLoLS decreases from 2.38 to 1.76. Similarly, the load shedding-based

TABLE IX
SLoLS WITH DIFFERENT LOAD MANAGEMENT STRATEGIES AND SWITCHABLE LINES

σ=20%, τ=0, υ=0				σ=20%, ξ=30%, υ=0				σ=20%, ξ=30%, τ=5%			
ξ	F	k=1	k=2	τ	F	k=1	k=2	υ	F	k=1	k=2
0	2.38	2.56	2.38	0	2.22	2.24	2.22	0	2.11	2.11	2.11
10%	2.28	2.41	2.28	5%	2.11	2.11	2.11	5%	1.76	1.76	1.76
20%	2.23	2.30	2.23	10%	2.01	2.01	2.01	10%	1.43	1.43	1.43
30%	2.22	2.24	2.22	15%	1.92	1.92	1.92	15%	1.11	1.11	1.11
40%	2.21	2.22	2.21	20%	1.83	1.83	1.83	20%	0.85	0.85	0.85
Time(s)	986	101	270	Time(s)	2702	322	595	Time(s)	442	78	268

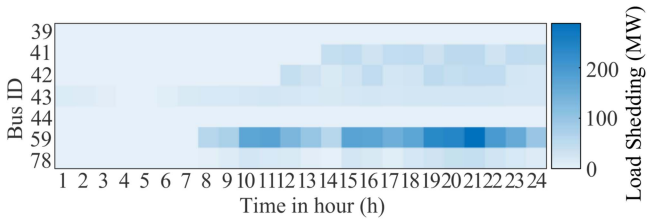

Fig. 6. Load shedding results of SLoLS based method.

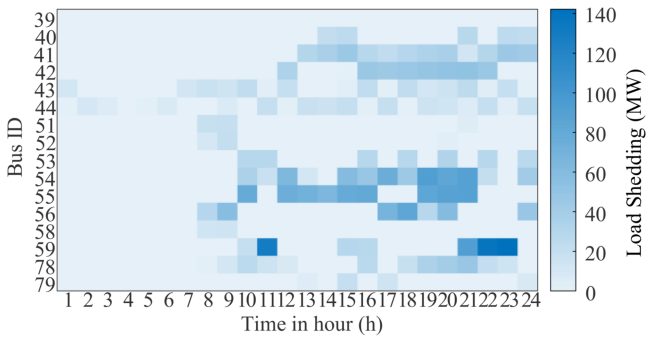

Fig. 7. Load shedding results of load shedding based method.

approach results in a decreasing trend in the volume of load shedding and SLoLS, in which load shedding decreases from 5899 MWh to 4290 MWh and SLoLS decreases from 3.12 to 2.59. Comparison of the load shedding and SLoLS results of different methods for the same scenarios indicates that the load shedding of the proposed model is slightly higher than that of the load shedding-based model. However, the SLoLS of the proposed method is lower than that of the load shedding-based method.

The specific load shedding schemes for each period are shown in Figs. 6 and 7. The load shedding schemes given by the two models have large differences. In terms of the number of buses with load shedding, six buses in the SLoLS-based method have shed load (buses 39, 41, 42, 43, 44, 59, and 78), and 16 buses show shedding in the load shedding-based method. Given the difference in the load shedding schemes, the SLoLS of the proposed method is only 1.76, which is 32.05% lower than that of the load shedding-based method.

2) Sensitivity Analysis of Different Load Management Measures: This section quantifies the impacts of different load management measures on reducing typhoon damages in consideration of OTS. It also analyzes the effectiveness of the OTS switchable line identification method in improving computational efficiency while ensuring solution accuracy. Three cases are considered in this session. 1) $k = 1$, 1-order correlation with the faulty lines; 2) $k = 2$, 2-order correlation with the faulty lines; 3) F, all transmission lines are taken as switchable lines.

According to the results in Table IX, the solving time decreases on the average by 9.7, 8.4, and 5.7 times for $k = 1$ in the three cases mentioned above, and the computational accuracy decreases slightly with a maximum error of 7.6% ($\sigma = 20\%$ and $\xi = \tau = \upsilon = 0$). The errors can be reduced with the increase in the demand-side management measures, and the results are the same in several scenarios when all lines of OTS are considered. When $k = 2$, the results show that SLoLS is exactly the same as that when all lines involved in OTS are considered, which indicates that all lines that can affect SLoLS at $k = 2$ are included. In terms of solution efficiency, the solving time decreases by 3.6, 4.5, and 1.6 times on the average for the three cases.

TABLE X
CHANGES IN NUMBER OF INTEGER VARIABLES AND CONSTRAINTS IN DIFFERENT CASES

k	1	2
Reduced number of binary variables	3384	2880
Reduced number of MILCs	13536	11520
Increased number of LCs	10152	8640
Total number of binary variables in case F	5856	
Total number of MILCs in case F	27984	

Table X the changes in the number of integer variables and constraints when k = 1/2 compared with all lines. From this result, the proposed method not only reduces the number of constraints but also transforms MILCs to LCs. When k = 1/2, the number of binary variables decreased by 57.79% and 49.18%, and the MILCs decreased by 48.37% and 41.17%, respectively. Although the total number of constraints does not decrease significantly with the increase in the number of LCs, the constraint types have undergone significant changes, with a large number of MILCs being transformed into LCs, which is also conducive to the rapid solution of the model. Transmission congestion can be effectively reduced by performing OTS on the lines near faulty lines. Accordingly, the number of lines involved in OTS is reduced, and the number of binary variables in the optimization model is decreased, which in turn improves the computing efficiency of the model.

TABLE XI
OTS RESULTS IN CASE K = 2 WITH SCENARIO $\sigma = 20\%, \xi = 30\%, \tau = 5\%, \upsilon = 5\%$

t	Switched Lines	t	Switched Lines	t	Switched Lines
1	35-37; 49-51; 46-47; 46-48; 68-69	9	42-49; 33-37; 19-34; 65-68; 47-69	17	49-66; 46-47; 46-48; 65-68; 68-69
2	54-59; 56-59; 64-65; 45-46; 65-68	10	42-49; 42-49; 69-77; 30-38; 68-69	18	47-49; 49-66; 19-34; 46-48
3	49-54; 38-37; 63-59; 69-77; 69-70	11	19-34; 30-38; 46-48; 65-68; 68-69	19	54-55; 63-59; 30-38; 46-47; 46-48
4	56-59; 56-59; 49-66; 49-66; 45-46	12	49-66; 69-77; 46-47; 46-48; 68-69	20	47-49; 69-77; 30-38; 46-48
5	49-66; 30-38; 38-65; 62-66; 65-68	13	47-49; 49-66; 49-66; 30-38; 46-48	21	47-49; 61-62; 64-65; 19-34; 46-48
6	42-49; 49-54; 56-57; 19-34; 45-46	14	47-49; 54-55; 63-59; 19-34; 46-47	22	33-37; 46-47; 46-48; 68-69; 69-70
7	49-54; 55-59; 69-75; 45-46; 62-67	15	49-69; 15-33; 30-38; 46-48; 68-69	23	54-59; 56-59; 64-65; 69-77; 47-69
8	55-59; 46-47; 47-69; 68-69	16	47-49; 30-38; 46-48; 65-66; 68-69	24	38-37; 47-49; 49-69; 46-47; 46-48

Morever, the OTS schemes in case $k = 2$ with scenario ($\sigma = 20\%$, $\xi = 30\%$, $\tau = 5\%$, $\nu = 5\%$) are shown in Table XI. Owing to space limitations, only the results from one case are listed here. OTS belongs to MILP, which has multiple solutions. Therefore, the transmission line switch on/off schemes obtained in different cases may differ even when the objective function values are the same.

V. CONCLUSION

To improve the capacity for important load preservation under typhoon disasters, this study proposes a preventive scheduling method of collaborative source–network–load resilience resources. Many active measures are implemented for the transmission network to optimize the transmission topology, improve the power flow distribution of lines, and give priority to the load with high priority. From the perspective of reducing the complexity of the OTS model, an effectiveness identification method of participating OTS switchable lines is proposed. The utility function of load shedding is defined by a power function, and a new index called SLoLS that considers the load composition in each bus is used to quantify the resilience of power systems. On this basis, a novel preventive scheduling method based on the utility function is developed by considering the load priority and the nonlinearity between losses and the amount of load shedding to minimize SLoLS. Auxiliary variables are introduced to transform the model into a mixed-integer linear formulation. The numerical results show that the proposed method can effectively improve power systems' resilience during typhoon disasters compared with the conventional method with the aim of minimizing the total amount of load shedding without considering load priority. During typhoon disasters, by adopting highly aggressive defensive strategies,

OTS can effectively improve the capacity for critical load preservation. Using the proposed switchable line effectiveness identification method can improve solution efficiency while ensuring model accuracy. In addition, switching on/off the lines near the fault location can effectively improve the supply capacity of important loads and reduce losses, which means that the lines located near the fault can serve as a set of OTS switchable lines to enhance the system's resilience.

In the future, the utility function-based power outage loss evaluation method can be further applied to power system planning and reinforcement model, and methods of improving power system resistance to typhoon disasters can be studied from the perspective of pre-disaster prevention through resource allocation with the aim to minimize SLoLS. In addition, to avoid the situation of multiple solutions, the differences in the switching on/off costs of different lines can be considered in the future.

REFERENCES

[1] Y. Wang, L. Huang, M. Shahidehpour, L. L. Lai, and Y. Zhou, "Impact of cascading and common-cause outages on resilience-constrained optimal economic operation of power systems," *IEEE Trans. Smart Grid*, vol. 11, no. 1, pp. 590–601, Jan. 2020.
[2] T. Zhao, H. Zhang, X. Liu, S. Yao, and P. Wang, "Resilient unit commitment for day-ahead market considering probabilistic impacts of hurricanes," *IEEE Trans. Power Syst.*, vol. 36, no. 2, pp. 1082–1094, Mar. 2021.
[3] C. Wang, Y. Hou, F. Qiu, S. Lei, and K. Liu, "Resilience enhancement with sequentially proactive operation strategies," *IEEE Trans. Power Syst.*, vol. 32, no. 4, pp. 2847–2857, Jul. 2017.
[4] H. Zhang et al., "Coordinated scheduling of generators and tie lines in multi-area power systems under wind energy uncertainty," *Energy*, vol. 222, May 2021, Art. no. 119929.
[5] G. Huang, J. Wang, C. Chen, J. Qi, and C. Guo, "Integration of preventive and emergency responses for power grid resilience enhancement," *IEEE Trans. Power Syst.*, vol. 32, no. 6, pp. 4451–4463, Nov. 2017.
[6] Y. Ge, L. Du, and H. Ye, "Co-optimization approach to post-storm recovery for interdependent power and transportation systems," *J. Modern Power Syst. Clean Energy*, vol. 7, no. 4, pp. 688–695, Jul. 2019.
[7] H. Zhang, H. Cheng, and S. Zhang, "Stochastic optimal transmission switching considering the correlated wind power," *IET Gener., Transmiss. Distrib.*, vol. 13, no. 13, pp. 2664–2672, Jun. 2019.
[8] K. Garifi, E. S. Johnson, B. Arguello, and B. J. Pierre, "Transmission grid resiliency investment optimization model with SOCP recovery planning," *IEEE Trans. Power Syst.*, vol. 37, no. 1, pp. 26–37, Jan. 2022.
[9] H. Zhang, S. Zhang, H. Cheng, G. Li, X. Zhang, and Z. Li, "Enhancing power grid resilience against typhoon disasters by scheduling of generators along with optimal transmission switching," in *Proc. IEEE/IAS Ind. Commercial Power Syst. Asia*, 2022, pp. 1725–1730, doi: 10.1109/ICPSAsia55496.2022.9949900.
[10] Y. Sang, J. Xue, M. Sahraei-Ardakani, and G. Ou, "An integrated preventive operation framework for power systems during hurricanes," *IEEE Syst. J.*, vol. 14, no. 3, pp. 3245–3255, Sep. 2020.
[11] L. Gong, Y. Fu, M. Shahidehpour, and Z. Li, "A parallel solution for the resilient operation of power systems in geomagnetic storms," *IEEE Trans. Smart Grid*, vol. 11, no. 4, pp. 3483–3495, Jul. 2020.
[12] G. Huang, J. Wang, C. Chen, J. Qi, and C. Guo, "Integration of preventive and emergency responses for power grid resilience enhancement," *IEEE Trans. Power Syst.*, vol. 32, no. 6, pp. 4451–4463, Nov. 2017.
[13] Z. Liu and L. Wang, "Leveraging network topology optimization to strengthen power grid resilience against cyber-physical attacks," *IEEE Trans. Smart Grid*, vol. 12, no. 2, pp. 1552–1564, Mar. 2021.
[14] C. Wang et al., "A systematic review on power system resilience from the perspective of generation, network, and load," *Renewable Sustain. Energy Rev.*, vol. 167, Jul. 2022, Art. no. 112567.

[15] J. M. Home-Ortiz, O. D. Melgar-Dominguez, M. S. Javadi, J. R. S. Mantovani, and J. P. S. Catalão, "Improvement of the distribution systems resilience via operational resources and demand response," *IEEE Trans. Ind. Appl.*, vol. 58, no. 5, pp. 5966–5976, Sep./Oct. 2022.
[16] R. Ashrafi et al., "Multi-objective resilience enhancement program in smart grids during extreme weather conditions," *Int. J. Elect. Power Energy Syst.*, vol. 129, Feb. 2021, Art. no. 106824.
[17] H. Azarinfar et al., "Modelling of demand response programs in energy management of combined cooling, heat and power-based microgrids considering resiliency," *IET Renewable Power Gener.*, vol. 17, no. 4, pp. 964–981, Dec. 2022.
[18] H. Ren et al., "Integrated optimization of a regional integrated energy system with thermal energy storage considering both resilience and reliability," *Energy*, vol. 261, Sep. 2022, Art. no. 125333.
[19] M. Alhazmi, P. Dehghanian, S. Wang, and B. Shinde, "Power grid optimal topology control considering correlations of system uncertainties," *IEEE Trans. Ind. Appl.*, vol. 55, no. 6, pp. 5594–5604, Nov./Dec. 2019.
[20] M. Khanabadi, Y. Fu, and C. Liu, "Decentralized transmission line switching for congestion management of interconnected power systems," *IEEE Trans. Power Syst.*, vol. 33, no. 6, pp. 5902–5912, Nov. 2018.
[21] M. Carrion and J. M. Arroyo, "A computationally efficient mixed-integer linear formulation for the thermal unit commitment problem," *IEEE Trans. Power Syst.*, vol. 21, no. 3, pp. 1371–1378, Aug. 2006.
[22] X. Liu et al., "A planning-oriented resilience assessment framework for transmission systems under typhoon disasters," *IEEE Trans. Smart Grid*, vol. 11, no. 6, pp. 5431–5441, Nov. 2020.
[23] T. Ding, M. Qu, Z. Wang, B. Chen, C. Chen, and M. Shahidehpour, "Power system resilience enhancement in typhoons using a three-stage day-ahead unit commitment," *IEEE Trans. Smart Grid*, vol. 12, no. 3, pp. 2153–2164, May 2021.
[24] C. Grigg et al., "The IEEE reliability test system-1996: A report prepared by the reliability test system task force of the application of probability methods subcommittee," *IEEE Trans. Power Syst.*, vol. 14, no. 3, pp. 1010–1020, Aug. 1999.
[25] H. Zhang, Jul. 22, 2023. [Online]. Available: https://github.com/hengzhangEE/The-modified-IEEE-two-area-system-and-the-IEEE-118-system
[26] Elect. Comput. Eng. Dept., Illinois Inst. Technol., Nov. 11, 2023. [Online]. Available: http://motor.ece.iit.edu/data/IEEE118bus_inf

Heng Zhang (Member, IEEE) received the B.S. degree in electrical engineering from China Agricultural University, Beijing, China, in 2014, and the Ph.D. degree in electrical engineering from Shanghai Jiao Tong University, Shanghai, China, in 2019. He is currently an Assistant Researcher with Shanghai Jiao Tong University. His research interests include power system planning and economic dispatch.

Shenxi Zhang (Senior Member, IEEE) received the B.S. degree in electrical engineering from Hohai University, Nanjing, China, in 2011, and the Ph.D. degree in electrical engineering from Shanghai Jiao Tong University, Shanghai, China, in 2016. He is currently an Associate Professor with Shanghai Jiao Tong University. His research interests include power system optimization, renewable generation, and integrated energy system.

Fangping Chen received the B.S. degree in electronics engineering from China Agricultural University, Beijing, China, in 2014, and the Ph.D. degree in computer science from Peking University, Beijing, China, in 2022. He is currently a Professor of Engineering with Wukong Lab, IKINGTEC Company, Ltd., Beijing, China. His research interests include artificial intelligence and its application in power systems.

Zheng Li received the B.S. and M.S. degrees in electrical engineering from China Agricultural University, Beijing, China, in 2014, and 2016, respectively. He is currently with State Grid Jiangsu Electric Power Research Institute. His research interests include power system planning and economic dispatch.

Haozhong Cheng received the M.S. and Ph.D. degrees in electrical engineering from Shanghai Jiao Tong University, Shanghai, China, in 1986 and 1998, respectively. He is currently a Professor with Shanghai Jiao Tong University. His research interests cover power system and integrated energy system planning.

Gang Li received the Ph.D. degrees in electrical engineering from Shanghai Jiao Tong University, Shanghai, China, in 2000. He is currently with East China Branch of State Grid, Shanghai, China. His research interests include power system planning and economic dispatch.

Xiaohu Zhang received the Ph.D. degree in electrical engineering from Shanghai Jiao Tong University, Shanghai, China, in 2013. He is currently with East China Branch of State Grid, Shanghai. His research focuses on power system planning.